JOURNAL of
MATERIALS and MECHATRONICS:A

e-ISSN 2717-8811
JournalMM, 2023, 4(1), 244-256
https://doi.org/10.55546/jmm.1257453

Araştırma Makalesi / Research Article

Parametric Optimization of Cutting Force and Temperature in Finite Element Milling of AISI P20 Steel

Rüstem BİNALİ*

Selçuk Üniversitesi, Teknoloji Fakültesi, Makine Mühendisliği Bölümü, Konya, Türkiye,
ORCID ID: https://orcid.org/0000-0003-0775-3817, rustem.binali@selcuk.edu.tr

Geliş/ Received: 27.02.2023; **Kabul / Accepted:** 10.04.2023

ABSTRACT: Multiple manufacturing methods are used in the manufacturing industry. The most commonly used method is machining methods. With machining methods, production can be made from both raw materials and finishing processes can be applied to products produced with different production methods. However, the initial cost of machining operations is quite high due to factors such as the machining parameters used during the process, the rigidity of the machine, and the machining conditions. Today, the finite element method (FEM) has been widely used in order to reduce the initial cost of machining. For this reason, in our study, the machining of AISIP20 material was carried out with the FEM. This study, four different cutting speeds, feed rates and two different cutting depths were used and the lateral feed rate was kept constant. As a result of the study, the cutting force values and temperature values that occurred depending on the machining parameters were evaluated by finite element analysis. Consequently, in the study, an increase in the cutting force occurred in general with the increase of feed, cutting depth and cutting speed parameters, and a decrease in temperature values occurred with an increase in cutting speed and feed and constant cutting depth. The lowest cutting force was 36.11 N, while the highest was 1951.42 N. The lowest and highest temperature values that occur during the process are 448.98 and 593.14 °C, respectively. In this regard, for the optimization of the parameters, the proportional change between the parameters and the finite elements as well as the physical processes can be performed for the desired final product.

Keywords: Milling, AISI P20, Finite elements, Cutting force, Temperature

*Sorumlu yazar / Corresponding author: rustem.binali@selcuk.edu.tr

Bu makaleye atıf yapmak için /To cite this article

Binali, R. (2023). Parametric Optimization of Cutting Force and Temperature in Finite Element Milling of AISI P20 Steel. Journal of Materials and Mechatronics: A (JournalMM), 4(1), 244-256.

1. INTRODUCTION

Today, cutting parameters and suitable cutting tools must be determined for machining operations especially for cutting of mixed geometries materials with high machining speeds (Kuntoğlu et al., 2020). The mechanical characteristics of the cutting tool play a significant role on the material removing performance from the surface and chip formation mechanism. In addition, the cutting strategy such as the environmental and physical properties of machine tool are also important. Therefore, the machining parameters and conditions of the materials should be selected properly (Demir et al., 2018; Salur, 2022). Machining parameters are not only effective on chip removal, but also on cutting forces, temperature, torque and roughness during and after machining. These cutting parameters are feed, cutting speed and cutting depth (Kuntoğlu and Sağlam, 2019; Binali et al., 2022). Irregular changes in the specified parameters will cause increased wear and poor surface quality due to cutting forces and temperatures. For this reason, it is imperative to select the optimal levels of cutting parameters considering the type of the material (Saglam et al., 2006; Demir et al., 2018). Physical experiments can be performed to determine optimum processing conditions and parameters. However, the high cost of physical experiments directs researchers to alternative experimental studies. These studies are numerical models and are widespread today. The commonly used numerical modeling method is the finite element method (Günay et al., 2016; Korkmaz and Günay, 2018). With this method, tests can be carried out to explore the mechanical characteristics and service conditions of utilized samples as well as the machining operations. Process outputs such as cutting force, temperature, moment, power consumption obtained in physical machinability experiments can be easily determined by the finite element method (Korkmaz and Günay, 2018; Binali et al., 2021;Binali et al., 2022).

According to the literature review, machinability tests of many materials have been carried out for machining parameters with the finite element method, taking into account the process outputs. Zhang et al. focused a three-dimensional FEM for the estimation of cutting forces in the course of hard milling of AISI H13 steel (Zhang et al., 2017). Li et al. have worked on the simulation and experimentation of chip analysis in the course of hard milling processes (Li et al., 2019). Gök, in his study, compared the temperature and cutting forces values that occur by turning AISI 1045 with both FEM and physical (Gok, 2015). Yaşar et al. investigated the cutting forces in the course of turning process of AISI P20 steel as numerical and experimental analysis (Günay et al., 2016). Korkmaz and Günay studied the consumed energy and cutting force machinability of AISI 420 Martensitic steel with FEM (Korkmaz and Günay, 2018). Özlü and Uğur investigated the optimization of cutting forces in turning of Ti-6Al-4V alloy with FEM (Ozlu and Ugur, 2021). Özçelik and Bağcı investigated drilling processes with helical drill cutting tools using experimental and finite element methods. They emphasized that there is a similarity between the analyzes made according to FEM and the results of the physical experiment performed under dry conditions (Ozcelik and Bagci, 2006). Ucun and Aslantaş studied the effects of two different coatings on cutting forces, stress of tool and temperature in the machining of AISI 4340 steel with 2D-thermoviscoplastic cutting simulation (Ucun and Aslantas, 2011). In his study, Özel stated that the physical tests and FEM simulation results were similar in terms of cutting force in the machining of PCBN cutting tools with variable cutting edge form and AISI 4340 steel, and there was an improvement in surface integrity and tool life due to low heat generation and stress concentration (Özel, 2009). Galanis and Manolakos studied finite element modeling to predict cutting forces when turning AISI 316L. The physical tests cutting force values were compared with the numeric results and it was concluded that they can be estimated with good accuracy with FEM (Galanis and Manolakos, 2014). Binali et al., in their study, optimized the machinability parameters of S960QL material using the FEM (Binali et al., 2021).

The aim of the study is to show that machinability tests can be done using the finite element method and it shows that physical tests can be reduced. In this study, AISI P20 mold steel was chosen as the workpiece material and TiAlN coated cemented carbide cutting tool was selected as the cutting tool to investigate the temperatures and cutting forces. Steels used in the molding industry are usually heat treated after processing for higher hardness. In this way, it is purpose to increase the resistance and high strength of the molds used at high temperatures. For this reason, it is desired that the process outputs do not damage the material before hardening process. In the literature search, it has been determined that there are studies on AISI P20, but it has been determined that the milling with the FEM is insufficient for the purpose of the article, and this study will shed light on the studies to be made on this material.

2. MATERIALS AND METHODS

Machinability tests were carried out using the FEM. The dimensions of workpiece samples used in the simulations are 25x25x50 mm in size. The chemical content of AISI P20 material is given in Table 1. The cutting tool used in the study was supplied by manufacturer's recommendations (AOMT123608PEER-M). During the experiments, four different cutting speeds and feeds and two different cutting depths were used. Table 2 summarizes the experimental parameters used in the experiments.

Table 1. Chemical content of AISI P20 (ASTM, 2022)

C wt%	Cr wt%	P wt%	Mn wt%	Si wt%	S wt%	Mo wt%
0.40	2.00	0.03	1.00	0.8	0.03	0.55

Table 2. Experimental parameters

Parameters	1. Level	2. Level	3. Level	4. Level
V (m/min)	170	200	230	270
f (mm/tooth)	0.075	0.113	0.169	0.253
a (mm)	0.75	1.50	-	-

Johnson-Cook (JC) parameters are required for the processing of AISI P20 material in the finite element method. The model equation used is given in equation 1 (Korkmaz and Günay, 2018). These parameters were derived from work by Shatla et al. (Shatla et al., 2001). JC model parameters are given in Table 3. The schematic representation of the simulation view is shown in Figure 1.

$$\sigma^0 = (A + B(\varepsilon^p)^n(1 + Cln\left(\frac{\dot{\varepsilon}^p}{\dot{\varepsilon}_0}\right))(1 - (\hat{T})^m) \quad (1)$$

Table 3. JC model parameters

A (Mpa)	B (MPa)	c	n	m	T_m
145	565.5	0.03	0.154	1.8	1753

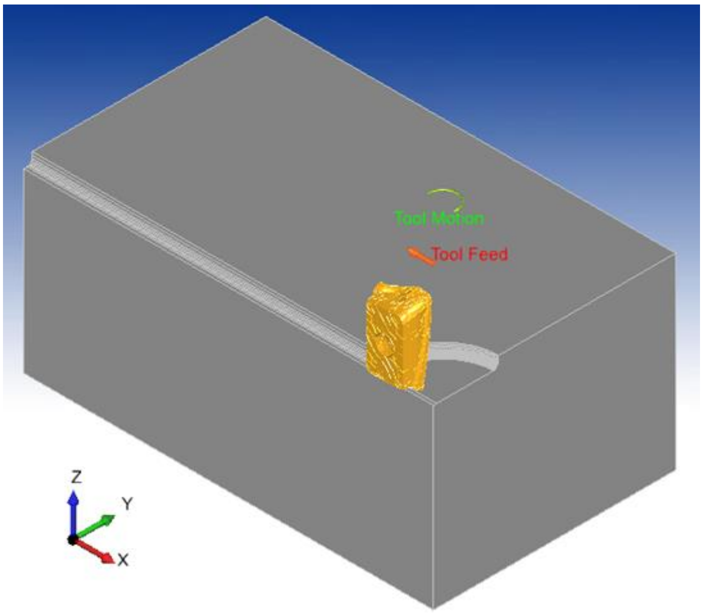

Figure 1. Schematic view

3. RESULTS AND DISCUSSION

In this section, the results of temperature and cutting force values will be discussed by considering simulation, optimization and analysis approaches. In this way, Taguchi S/N ratios for optimization, ANOVA and graph plot analysis for the results of cutting forces and temperatures obtained from simulation will be performed.

3.1 Optimization with Taguchi S/N Ratios for Finite Element Modelling Results

Taguchi is extensively applied to experimental design and optimization for engineering problems (Zhang et al., 2007; Binali et al., 2022; Binali et al., 2022). Taguchi uses an objective function to determine the optimum parameters in a set of input parameters. In this way, it is tried to ensure that the outputs are at the desired level (Ghani et al., 2004). Taguchi basically aims to reduce the processing costs and the energy and labor consumed by limiting the number of experiments. In addition, it is desired to reach high quality in a shorter time. There are three types of objective functions: smaller better, nominal best, and larger better. In this study, the smaller the better type of target function was used to obtain as minimal cutting forces as possible. The levels, design and result values of the parameters used in the study are given in Table 4.

Table 4. Experimental design and results

a (mm)	f (mm/tooth)	V (m/min)	Temperature	Force component-X (N)	Force component-Y (N)	Force component - Z (N)
1	1	1	532.89	85.18	685.81	311.33
1	2	1	593.14	187.84	929.33	358.10
1	3	1	518.07	411.02	1218.22	446.82
1	4	1	504.95	381.27	836.10	386.88
1	1	2	460.13	138.51	735.44	300.29
1	2	2	478.83	143.11	940.41	384.35
1	3	2	520.48	325.98	1053.02	365.30
1	4	2	532.41	434.79	857.12	398.31
1	1	3	476.40	149.18	793.32	315.75
1	2	3	492.96	188.72	1034.98	416.53
1	3	3	523.79	344.47	1134.95	409.62
1	4	3	557.87	422.87	836.40	387.08
1	1	4	544.04	129.89	695.54	297.49
1	2	4	501.73	205.40	795.31	295.99
1	3	4	578.54	400.10	1216.16	502.68
1	4	4	547.87	375.63	842.06	394.99
2	1	1	448.98	-38.40	1094.42	239.21
2	2	1	478.11	193.52	1399.53	262.47
2	3	1	509.79	327.59	1951.42	393.95
2	4	1	494.62	548.82	1649.94	227.92
2	1	2	476.23	38.76	1076.57	235.89
2	2	2	494.98	238.23	1796.54	271.76
2	3	2	523.55	366.45	1457.72	203.59
2	4	2	512.53	653.42	1890.40	341.58
2	1	3	492.93	36.11	1090.53	249.30
2	2	3	510.63	339.45	1787.93	248.07
2	3	3	529.23	219.45	1936.73	281.72
2	4	3	565.43	694.02	1676.46	316.42
2	1	4	515.13	45.35	1121.51	221.77
2	2	4	548.04	166.79	1622.69	234.06
2	3	4	540.79	408.91	1886.80	301.81
2	4	4	518.00	746.71	1769.25	344.32

To find out the optimal points of the milling variables used this the study, the determined S/N ratios are given in Tables 5, 6, 7 and 8.

Table 5. Signal to noise ratios of X axis cutting force component

Level	V	f	a
1	**-46.31**	**-36.87**	-47.58
2	-46.98	-46.09	**-46.38**
3	-47.21	-50.75	-
4	-47.42	-54.22	-
Delta	1.10	17.36	1.20
Rank	3	1	2

By examining the data in Table 5, the effects of milling parameters on X-axis cutting force are feed rate, depth and speed, respectively. Ideal machining parameters are first feed rate and speed and second level of depth.

Table 6. Signal to noise ratios of Y axis cutting force component

Level	V	f	a
1	**-61.26**	**-59.01**	**-59.07**
2	-61.31	-61.80	-63.76
3	-61.73	-63.16	-
4	-61.34	-61.67	-
Delta	0.47	4.15	4.69
Rank	3	2	1

By examining the data in Table 6, the effects of milling parameters on the Y-axis cutting force are feed rate, speed and depth respectively. The ideal cutting parameters are first of feed rate, speed and depth.

Table 7. Signal to noise ratios of Z axis cutting force component

Level	V	f	a
1	-50.09	**-48.59**	-51.34
2	**-49.69**	-49.62	**-48.59**
3	-50.15	-50.90	-
4	-49.94	-50.75	-
Delta	0.47	2.31	2.75
Rank	3	2	1

By examining the data in Table 7, the effects of milling parameters on the Z-axis cutting force are cutting depth, speed and feed rate, respectively. Ideal machining parameters are second level of the speed and depth along with first level of feed.

Table 8. Average S//N response for the temperature

Level	V	f	a
1	-54.13	**-53.84**	-54.35
2	**-53.97**	-54.17	**-54.14**
3	-54.28	-54.49	-
4	-54.59	-54.46	-
Delta	0.62	0.64	0.21
Rank	2	1	3

By examining the data in Table 8, the effects of machining parameters on the cutting temperature in the course of the process are feed, cutting speed and cutting depth, respectively. Ideal machining parameters are 2nd of the V and depth and 1st of the f.

ANOVA analysis results obtained for cutting forces and temperature are given in Table 9, 10, 11 and Table 12.

Table 9. ANOVA for the X axis cutting force

	DoF	SS	MS	F-value	p value	PC (%)
V	3	6214	2071	0.24	0.864	0.55
f	3	896004	298668	35.29	0.000	79.83
a	1	17021	17021	2.01	0.169	1.52
Error	24	203120	8463			18.10
Total	31	1122359				

There are ANOVA analysis results of the parameters affecting the X-axis strength in Table 9. According to the results of the analysis, the effect values were respectively 79.83% feed rate, 1.52% cutting depth and 0.55% cutting speed. If we look at the significance levels, it can be said that the feed rate has an important effect on the X-axis force since the p value is less than 0.05.

Table 10. ANOVA for the Y axis cutting force

	DoF	**SS**	**MS**	**F-value**	**p value**	**PC (%)**
V	3	21392	7131	0.27	0.848	0.39
f	3	1372681	457560	17.21	0.000	24.75
a	1	3514079	3514079	132.15	0.000	63.36
Error	24	638176	26591			11.51
Total	31	5546327				

The parameters affecting the cutting force in Y-axis are listed in Table 10. According to the results of the analysis, these variables were observed respectively 63.36% for cutting depth, 24.75% for feed rate and 0.39% for cutting speed. If we look at the significance levels, it can be said that the amount of feed rate and the cutting depth have an important effect on the Y-axis force since the p values is less than 0.05.

Table 11. ANOVA for the Z axis cutting force

	DoF	**SS**	**MS**	**F-value**	**p value**	**PC (%)**
V	3	1300	433.4	0.21	0.892	0.75
f	3	41519	13839.6	6.56	0.002	23.97
a	1	79764	79764.5	37.82	0.000	46.05
Error	24	50618	2109.1			29.23
Total	31	173202				

ANOVA analysis results of the parameters affecting the Z-axis strength are given in Table 11. According to the results of the analysis, the effect values were 46.05% cutting depth, 23.97% feed rate and 0.75% cutting speed, respectively. If we look at the significance levels, it can be said that the amount of feed and the cutting depth have a significant effect on the Z-axis force since the p value is less than 0.05.

Table 12. ANOVA for the temperature

	DoF	**SS**	**MS**	**F-value**	**p value**	**PC (%)**	**DoF**
V	3	5860	5860	1953.4	2.36	0.096	17.07
f	3	7298	7298	2432.5	2.94	0.053	21.26
a	1	1315	1315	1314.8	1.59	0.219	3.83
Error	24	19849	19849	827.0			57.83
Total	31	34321					

As for temperature, the effecting parameters are given in Table 12. According to the results of the analysis, the effect values were respectively 21.26% feed rate, 17.07% cutting speed and 3.83% cutting depth.

In general, as a result of the evaluation of the ANOVA results, the least effect value on the cutting forces occurred at the cutting speed. In temperature values, the least effect occurred at the cutting depth. It has been concluded that the feed has the highest effect on cutting forces and temperature values.

3.2 Finite Elements Modelling Results for Cutting Force

In Figure 2 and Figure 3, cutting forces graphs are given at different depths of cut and depending on the variation of feed rate and cutting speed.

If we look at the cutting forces from a general point of view, an increase in cutting forces occurs as a result of increasing feed rates. It is seen that an increasing trend in cutting forces is visible with increasing depth. In addition, decreasing behavior for cutting forces were observed with the elevation of speed. But for some cases, decreasing trend for cutting forces were clear with the increase of feed and speed. This case can be explained by the material properties and specified cutting tool preferred in the experiments. In addition, the cause of the differences can be explained by the increased chip cross-sectional area and therefore the power required for the amount of chip removed from the material per unit time (Küçüktürk, 2013; Günay et al., 2018). This situation can also be explained by considering the reduced strength of the workpiece material with elevated temperature (Binali et al., 2021).

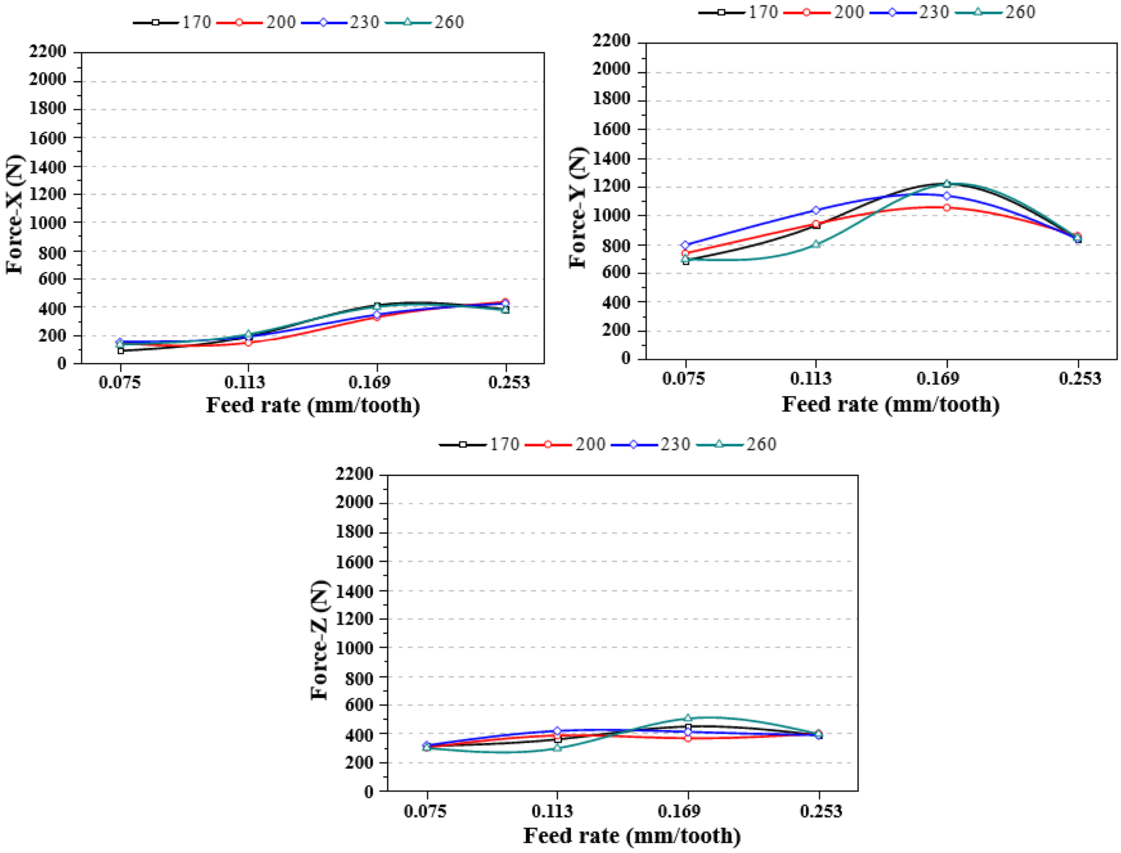

Figure 2. Cutting force graph based on feed and cutting speed at 0.75 mm cutting depth

As a result of the analysis of the graphics depending on the feed rate and cutting speeds, an increase in cutting forces occurs with an increase in the amount of feed in general. When evaluated according to cutting speeds, it is seen that the cutting force decreases with increasing cutting speeds and increases after a while with increasing feed rate. When the literature is examined, the increase in feed force increases the cutting force and the increase in cutting speed decreases the cutting force (Chinchanikar and Choudhury, 2013; Salur et al., 2020; Kuntoğlu et al., 2021). However, these explanations are used for turning and drilling experiments in the literature. Wavy results can occur because the cutting mechanics of the milling process are different from other methods (Binali, 2017). As a result of the evaluation of the data in Figure 2, the highest cutting force (1218.22 N) occurred in the Y axis direction with 0.169 mm/tooth f and 170 m/min V. The lowest force (85.18 N) value occurred in the X-axis direction at 0.075 mm/tooth f and 170 m/min V. A change of approximately 1330% occurred between the highest and lowest strengths.

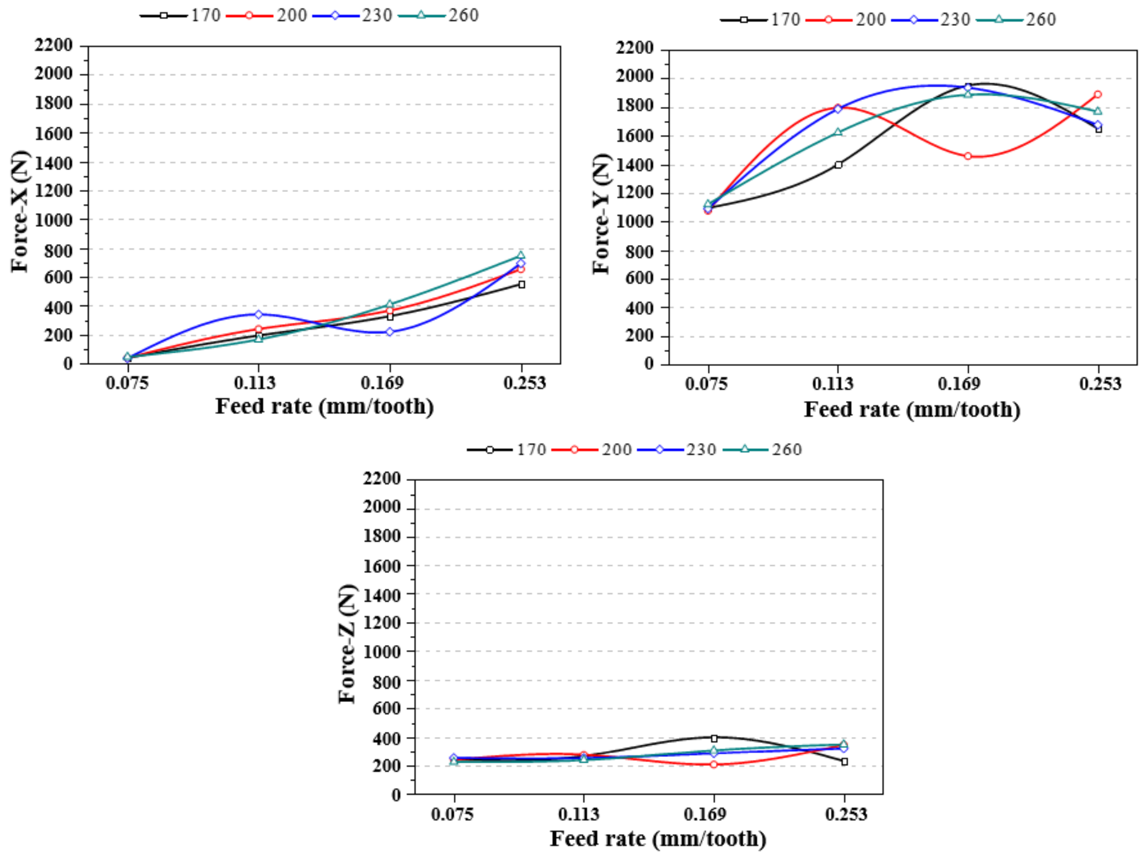

Figure 3. Cutting force graph based on feed and cutting speed at 1.5 mm cutting depth

Figure 3 shows the cutting force curves as a function of f and V values with the constant cutting depth at 1.5 mm. However, the fluctuating results were observed in cutting forces based on different cutting speeds. The highest cutting force (1951.42 N) occurred in the Y-axis direction with 0.169 mm/tooth f and 170 m/min V. The lowest cutting force (36.11 N) was monitored in the X-axis direction at 0.075 mm/tooth f and 230 m/min V. A change between the highest and lowest cutting force values were calculated as an approximately 5300%.

3.3 Finite Elements Modelling Results for Temperature

During machining tests, temperatures reveal in cutting area due to cutting forces and tribological contacts at the chip and tool faces. This temperature varies according to the workpiece, cutting tool, cutting parameters and conditions. This temperature causes wear on the material and tool, preventing the desired level of product being obtained. For this reason, it is necessary to optimize the temperature distributions according to the machining parameters in line with all these expressed information during machining. In Figure 4 and Figure 5, graphical evaluations of the temperature distributions formed during the process according to the 0.75 mm and 1.5 mm cutting depth are given.

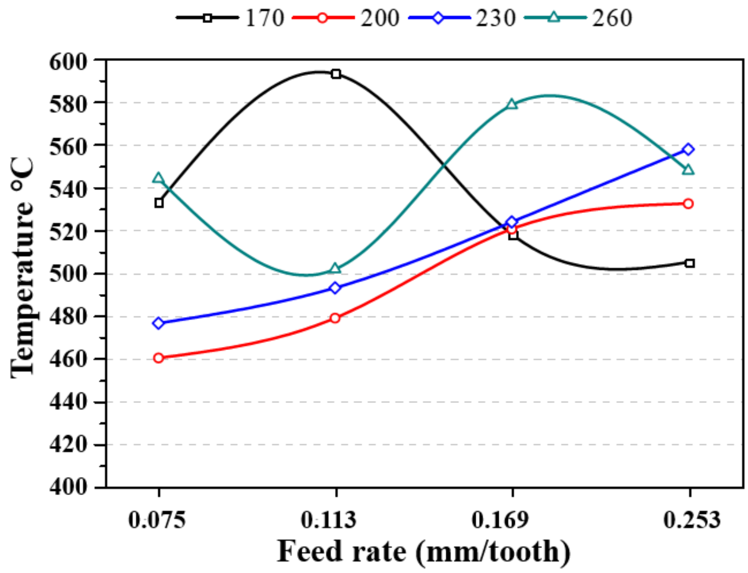

Figure 4. Temperature graph based on feed and cutting speed at 0.75 mm cutting depth

By examining the curves in Figure 4, an increase in the amount of temperature is observed depending on the constant V and the increasing f in the cutting depth. It is seen that there is a general increase in cutting temperatures with increasing V. The highest temperature value (593,14 °C) occurred at 0.75 mm cutting depth, 170 m/min V and 0.113 mm/tooth feed rate. The lowest temperature value (460,13 °C) occurred at 200 m/min V and 0.075 mm/tooth feed rate. A change of approximately 22.42% occurred between the highest and lowest temperature values.

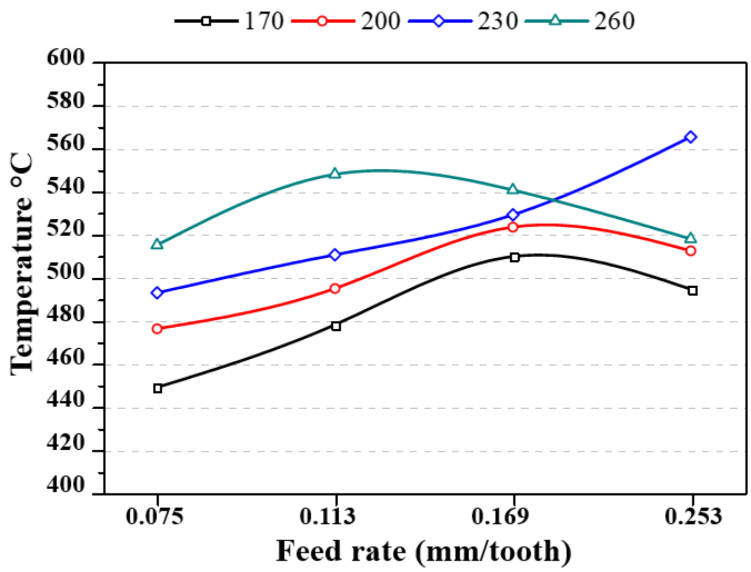

Figure 5. Temperature graph based on feed and cutting speed at 1.5 mm cutting depth

By examining the graph in Figure 5, an increase in temperature values occurred with increasing feed rate and cutting speed. This situation has occurred in accordance with the literature (Usca et al., 2021). According to the graph in Figure 5, the highest temperature value (565.43 °C) is 230 m/min V and 0.253 mm/tooth f, the lowest temperature value (448.98 °C) is 170 m/min V and 0.075 mm/tooth f. There is a change of approximately 20.59% between the highest and lowest temperature values.

4. CONCLUSION

The paper focused on the machinability of AISI P20 steel with the milling was investigated by evaluating the temperatures and cutting forces in the course of the process using the FEM. The results are given below.

- In general, increasing of feed and depth, the temperature and cutting force values also increased.
- The highest cutting force in the simulation results was 1951.42 N, at a cutting depth of 1.5 mm in the Y axis direction, 0.169 mm/tooth f and 170 m/min V. The lowest cutting force value was 36.11 N in the X-axis direction at 1.5 mm cutting depth, 230 m/min V and 0.075 mm/tooth f.
- The lowest temperature value in the simulation results was 448,98 °C at 1.5 mm cutting depth, 0.075 mm/tooth f and 170 m/min V. The highest temperature value was 593.14 °C at 0.75 mm cutting depth, 0.113 mm/tooth f and 170 m/min V.
- It has been concluded that milling with the FEM can be used for the estimation of machinability outputs.
- In the FEM, studies can be conducted on the analysis of process outputs such as moment and chip formation of different processes, materials and machining parameters with cutting tools.
- Comparison of machinability criteria can be made by using different finite element programs for machining operations.

5. CONFLICT OF INTEREST

Authors approve that to the best of their knowledge, there is not any conflict of interest or common interest with an institution/organization or a person that may affect the review process of the paper.

6. AUTHOR CONTRIBUTION

Rüstem BİNALİ has the full responsibility of the paper about determining the concept of the research, data collection, data analysis and interpretation of the results, preparation of the manuscript and critical analysis of the intellectual content with the final approval.

7. REFERENCES

ASTM, 2022. P20 Steel Plate, https://www.astmsteel.com/product/p20-steel-plate-1-2311-3cr2mo-mold-tool-steel/ (Date of access: 05.04.2022)

Binali R., Sıcak iş takım çeliğinin (TOOLOX 44) işlenebilirliğinin incelenmesi. Karabük Üniversitesi Fen Bilimleri Enstitüsü, Master Thesis (Printed), 2017.

Binali R., Coşkun, M., Neşeli, S., An Investigation of Power Consumption in Milling AISI P20 Plastic Mold Steel By Finite Elements Method. Avrupa Bilim ve Teknoloji Dergisi (34), 513-518, 2022.

Binali R., Yaldız, S., Neseli, S., Parametric optimization for machinability parameters of S960QL structural steel during milling by finite elements. Selcuk University Journal of Engineering Sciences 21(1), 26-31, 2022.

Binali R., Yaldız, S., Neşeli, S., S960QL Yapı Çeliğinin İşlenebilirliğinin Sonlu Elemanlar Yöntemi ile İncelenmesi. Avrupa Bilim ve Teknoloji Dergisi (31), 85-91, 2021.

Chinchanikar S., Choudhury S., Effect of work material hardness and cutting parameters on performance of coated carbide tool when turning hardened steel: An optimization approach. Measurement 46(4), 1572-1584, 2013.

Demir H., Ulaş H. B., Binali R., Toolox 44 malzemesinde talaş kaldırma miktarının yüzey pürüzlülüğü ve takım aşınması üzerindeki etkilerinin incelenmesi. Technological Applied Sciences 13(1), 19-28, 2018.

Galanis N., Manolakos D. E., Finite element analysis of the cutting forces in turning of femoral heads from AISI 316l stainless steel. In Proceedings of the World Congress on Engineering (Vol. 2), 2014.

Ghani J. A., Choudhury I., Hassan H., Application of Taguchi method in the optimization of end milling parameters. Journal of Materials Processing Technology 145(1), 84-92, 2004.

Gok K., Development of three-dimensional finite element model to calculate the turning processing parameters in turning operations. Measurement 75, 57-68, 2015.

Günay M., Meral T., Korkmaz M. E., AISI 420 Martenzitik paslanmaz çeliğin delinebilirliğinin sonlu elemanlar yöntemiyle analizi. Gazi Mühendislik Bilimleri Dergisi 4(3), 223-229, 2018.

Günay M., Yaşar N., Sekmen M., Korkmaz M. E., AISI P20 çeliğinin işlenmesinde kesme kuvvetinin deneysel ve nümerik analizi. Gazi University Journal of Science Part C: Design and Technology 4(1), 13-19, 2016.

Korkmaz M. E., Günay M., Finite element modelling of cutting forces and power consumption in turning of AISI 420 martensitic stainless steel. Arabian Journal for Science and Engineering 43(9), 4863-4870, 2018.

Kuntoğlu M., Acar O., Gupta M. K., Sağlam H., Sarikaya M., Giasin K., Pimenov D. Y., Parametric optimization for cutting forces and material removal rate in the turning of AISI 5140. Machines 9(5), 90, 2021.

Kuntoğlu M., Aslan A., Sağlam H., Pimenov D. Y., Giasin K., Mikolajczyk T., Optimization and analysis of surface roughness, flank wear and 5 different sensorial data via tool condition monitoring system in turning of AISI 5140. Sensors 20(16), 4377, 2020.

Kuntoğlu M., Sağlam H., Investigation of progressive tool wear for determining of optimized machining parameters in turning. Measurement 140, 427-436, 2019.

Küçüktürk G., Modeling and analyzing the effects of experimentally determined torque and thrust force on cutting tool according to drilling parameters. Proceedings of the Institution of Mechanical Engineers, Part B: Journal of Engineering Manufacture 227(1), 84-95, 2013.

Li B., Zhang S., Zhang Q., Li L., Simulated and experimental analysis on serrated chip formation for hard milling process. Journal of Manufacturing Processes 44, 337-348, 2019.

Ozcelik B., Bagci E., Experimental and numerical studies on the determination of twist drill temperature in dry drilling: A new approach. Materials & Design 27(10), 920-927, 2006.

Ozlu B., Ugur L., Optimization of cutting forces on turning of Ti-6Al-4V Alloy by 3D FEM simulation analysis. Journal of Engineering Research and Applied Science 10(2), 1789-1795, 2021.

Özel T., Computational modelling of 3D turning: Influence of edge micro-geometry on forces, stresses, friction and tool wear in PcBN tooling. Journal of Materials Processing Technology 209(11), 5167-5177, 2009.

Saglam H., Unsacar F., Yaldiz, S., Investigation of the effect of rake angle and approaching angle on main cutting force and tool tip temperature. International Journal of Machine Tools and Manufacture 46(2), 132-141, 2006.

Salur E., Understandings the tribological mechanism of Inconel 718 alloy machined under different cooling/lubrication conditions. Tribology International 174, 107677, 2022.

Salur E., Aslan A., Kuntoğlu M., Güneş A., Şahin Ö., Optimization of cutting forces during turning of composite materials. Acad. Platf. J. Eng. Sci. 8, 423-431, 2020.

Shatla M., Kerk C., Altan T., Process modeling in machining. Part I: determination of flow stress data. International Journal of Machine Tools and Manufacture 41(10), 1511-1534, 2001.

Ucun İ., Aslantas K., Numerical simulation of orthogonal machining process using multilayer and single-layer coated tools. The International Journal of Advanced Manufacturing Technology 54(9), 899-910, 2011.

Usca Ü. A., Uzun M., Kuntoğlu M., Sap E., Gupta M. K., Investigations on tool wear, surface roughness, cutting temperature, and chip formation in machining of Cu-B-CrC composites. The International Journal of Advanced Manufacturing Technology 116(9), 3011-3025, 2021.

Zhang J. Z., Chen J. C., Kirby E. D., Surface roughness optimization in an end-milling operation using the Taguchi design method. Journal of Materials Processing Technology 184(1-3), 233-239, 2007.

Zhang Q., Zhang S., Li J., Three dimensional finite element simulation of cutting forces and cutting temperature in hard milling of AISI H13 steel. Procedia Manufacturing 10, 37-47, 2017.